Talk: 25.10.2019
Submission: **.01.2020

Summary

Schlüsselexperimente der Teilchenphysik

Janina Nicolini[1]

[1]janina.nicolini@tu-dortmund.de

Contents

1 Cherenkov Detectors [1]

Cherenkov detectors are based on the fact that charged particles that travel faster a light in a medium emit light. The measured light can be used to reconstruct properties of the particles.

1.1 Theoretical principles

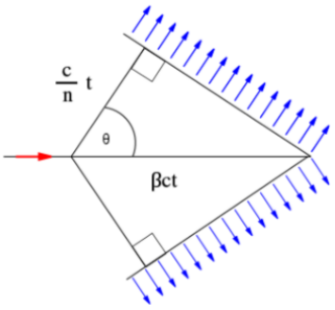

Figure 1: Schematic representation of the Cherenkov light cone. [1]

The speed of light in a medium is defined by $c = \frac{c_0}{n}$, where c_0 is the speed of light in vacuum and n the refractive index of the medium. If a charged particle travels lokally with $v_p > c$, it emits Cherenkov photons under a angle ϑ. This is caused by the relaxation of the polarization of a dielectric medium. Due to the high velocity of the particle an aysymmetric polarization of the medium is created, which then leads to a Mach cone. The angle is given by

$$\cos\vartheta = \frac{c/n\,t}{\beta\,c\,t} = \frac{1}{n\,\beta}\,.$$

The cherenkov radiation has a continuously spectrum with a maximum in the UV range. The intensity is approximately proportional to the frequency of light in the visible spectrum. This is the reason why Cherenkov radiation is usually seen as blue.
For Cherenkov light in the atmosphere there are usually two different sources. The first cone is produced by the original particle e.g. an iron nucleus and the second one by the particle shower produced due to the original particle.

1.2 Historical development

P. Cherenkov discovered the light around a radioactive preparation in water in 1934. I. Tamm and I. Frank developed the corresponding the theory in 1937. All theory were awarded with the Nobel prize for their work in 1958. The first Cherenkov counter was developed in 1951 and was used to detect cosmic rays with Cherenkov light in water. A cylinder with distilled water is used as the radiator and connected to a photomultiplier. Behind it there is preamplifier to increase the signals. Around the same time a so called getting type Cherenkov detector was designed. The radiator was a acrylic plastic cone with a top angle Φ. It is followed by a lens that only focus Cherenkov light that was emitted with $\vartheta = \Phi$ trough a collimeter and is afterwards measured by a photomultiplier.

1.3 Cherenkov detector types

Treshold Detectors were used in earlier collider experiments starting in 1951. They use specific mediums to distinguish differnent particles. The produced photons are beamed towards photomultipliers by using mirrors. The peak hight measured with the photomultiplier can be used to reconstruct the particle velocity. They made it possibe to distinguish between pions, kaons and protons. *Differential Cherenkov Detectors* use the angle of the Cherenkov cone together with a spherical mirror to focus the light trough a diaphragm. The radius of the diaphragm limits the measureable velocity range. Changing the preasure inside of the gas radiator controlls the refractive index. For this reason they are used to select particles instead of identifying them.
Ring Imaging Cherenkov Detectors (RICH) were first designed in 1976. They can be used to reconstruct the particle speed between $0.5 - 150\,\mathrm{GeV}$. At higher momentums it is not possible to distinguish the Cherenkov angles of different particles. They consist of a sperical detector (R_c) surrounded by a mirror(R) and the radiator is filled in between.

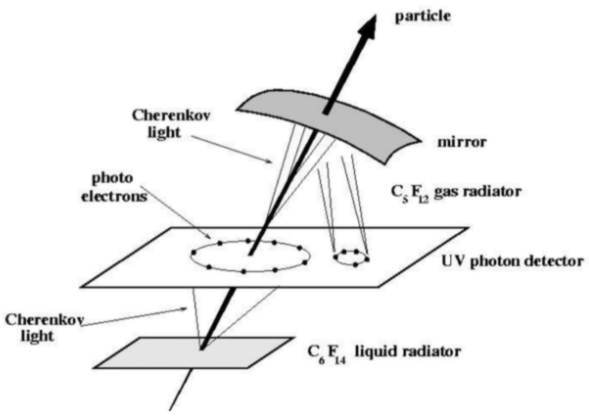

Figure 2: RICH detector in the DELPHI experiment using two radiators and one photon detector. The Cherenkov light is projected on both sides of the detector. [1]

The Cherenkov light is emitted in between the detector and the mirror and reflected on the photo detector. This reflection makes it possible to calculate the velocity with $\vartheta \approx 2\frac{R_c}{R}$. Current RICH detector work with two radiators this leads to a larger momentum range as shown in figure 2. The main challenge for the photo detector is that it must be able to localize the spatial positio in the ring image. The Cherenkov photons are transformed into photoelectrons and measured in a multiwire propotional chamber. This leads to the reconstruction of two coordinates, the last one can be calculated from the drift time of the electrons. *Detection of Internally Reflected Cherenkov light* (DIRC) is a principle where a pipe radiator is used to produce the Cherenkov light and guide it towards a light catcher. The angle information remains unchanged. This detector was used in the Babar experiment *Cherenkov Calorimeter* for example made out of lead glass as a radiator. The produced light is propotional to the energy of the entering charged particles. This technology was used for the electromagnetic calorimeter of the OPAL experiment.

The first *Imaging Atmospheric Cherenkov Telescopes* was developed by the whipple collaboration in the early 1980. They are able to detect high gamma ray showers in a range of 50 GeV to 50 TeV. A large segmented, spherical mirror is used to reflect the Cherenkov light onto an array of photomultipliers. Gamma showers are usually of elliptic shape, while hadronic interactions result in broader and irregular showers due to the larger transverse momentum. Usually the Cherenkov cones cover a size of several $100\,\mathrm{m}^2$ for this reason several telescopes are grouped together to cover as much of the shower as possible. A benefit of this is, that the angular resolutions increases with each added telescope. Projection all images into one plane allows to reconstruct the originial direction of the shower. IACT detectors lead for example to the discovery of the Crab nebula in 1989. Till today they provide the best measurements of angular and energy resolution in the TeV domain.

A special use of IACT detectors are *Neutrino Observatories*. The IceCUBE experiment is at the Amundsen-Scott South Pole Station in Antarctica. It consists of 86 photomultipliers that are symmetricly placed incide of a $1\,\mathrm{m}^3$ cube of ice. The ice functions as a radiator. If a neutrino reacts with the ice, it creates charged leptons that can radiate Cherenkov light. On the surface of the cube is IceTop, a detector with the purpose to detect cosmic particles and can then be used as veto for the IceCube Array. The DeepCore is build out of the 6 most inner photomultipliers, which are placed with a smaller distance. This is the reason why IceCUBE measures neutrinos in the range of 100 GeV to several PeV. Beside the reconstruction of the energy it is also possible to determine the original direction of the neutrinos. IceCUBE measured a non-terrestrial neutrino flux in 2013. One of the most recent discoveries were the identification of two high-energy neutrino sources. Super-Kamiokande is a cylindrical water tank with a volume of around $200\,000\,\mathrm{m}^3$. It is placed 1 km below the surface, uses the same principles as IceCUBE and the photomultipliers are positioned at the wall. Electrons produce a spheric Cherenkov ring, while the track of muons is much longer due to the slower energy loss. One of the most important discoveries of the Super-Kamiokande was the discovery of neutrino oszillation.

2 Semiconductor detectors [2]

Semiconductors are solid states with periodic lattice structure and their important feature is the size of their band gap. While they are isolator at a temperature of absolute zero, their conductivity grows exponentially with the temperature. This is due to the thermal energy being able to excite a valence electron into the conduction band.

2.1 Properties of semiconductors

For intrinsic semiconductors the conductivity is only given by the electron moving into the conduction band and the reminding hole in the valence band. They are interpretated as positive charge carrier. Real crystals usually have imperfections due to chemical impurities or structural defects, which slightly changes the properties.

Doping is a method where intentionally impurities are added to the lattice. This are usually atoms

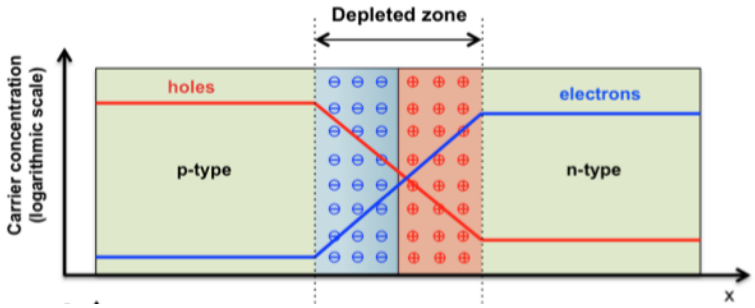

Figure 3: Diagram of the interference region of a p-n juntion. [3]

with an additional or one valence electron less to create n-doped (free electron) or p-doped (free hole) semiconductors. Adding a p- und n-doped Semiconductor together creates a p-n junction which is the base of all present semiconductor devices. Figure 3 shows a schematic representation of a p-n junction. Due to the different carrier concentrations, they start drifting into eachother and recombine. This creates the depletion zone, which does not contain any free charge carrier. Applying an external voltage to the p-n junction in reverse biasing (anode to the n-side, cathode to the p-side) enlarges the width of the depletion zone, while applying the forward-biasing (anode to the p-side, cathode to the n-side) decreases its width. The reverse biasing ensures that the semiconductor detector behaves like a diode. In this condition a small current flows until a breakdown voltage is reached. The best condition to use a semicondutor devise as detector is with a high enough voltage so the depletion zone occupies the whole sensor. This condition is called fully depleted and there are no free charge carriers present. If a charged particle crosses the fully depleted sensor, it leaves an ionization track which can be measured with the electronics at the surface of the semicondutor.

The leakage current is main background for the signal collected with a semiconductor detector. Its main source is thermally generated electron-hole pairs in the depletion zone. To decrease this leakage current the sensors are usually cooled.

The semiconductors have severeal advantages compared to gas chambers due to their properties. They have good tracking properties in terms of time and spatial resolution. They also have a rapid charge-collection of $\sim 10\,\text{ns}$ due to the higher density which makes them suitable for HEP experiment conditions. This also leads to a greater stopping power and allows to build thinner detectors. Another benefit is the ionization energy of just $\sim 3\,\text{eV}$ compared to $\sim 30\,\text{eV}$ for gas-based detectors. This leads to a better signal and energy resolution. The only significant downside is that they suffer a significant degradation from radiation-induced damage during their lifetime. The two mainly used materials are Silicon and Germanium. Germanium has a higher atomic number and therefore is better for γ-ray

detection. But due to the small band gap energy it needs cooling, while Silicon can be operated at room temperature. It is also cheaper and therefore the mainly used material at HEP detectors e.g. at the large hadron collider (LHC) experiments at CERN.

2.2 Historical development of semiconductor detectors

In 1949 K. G. McKay published a paper about a Germanium point-contact diode, which was the first semiconductor detector. In the 1960s monocrystalline siicone became aviable. In the 1970s Boyle and Smith published their concept for Charge-Couple Devices (CCD), which was later rewarded with the Nobel prize. J. Kemmer finally introduced the planar technology to build diodes and transitors in 1979. This was the revolution in silicon detectors leading to the advanced forms of strip and pixel sensors. The HEP experiments NA11-NA32 were then the first experiments using silicon microstrip sensor to c´study charm physics. In 1994 DELPHI installed the first silicon vertex detector. This principles are still being used at current HEP experiments with upgraded technologies.

2.3 Silicon detector technologies

Silicon Drift Detectors use the principle of sidewards depletion, where the electric field is parallel to the surface of the silicon waver. Hence the position is measured trough the drift time. There are also able to measure the energy of the ionising radiation. Different shapes of the electrodes allow flexible configuration e.g. matrix drift devices that allow to perform a 2D position measurement.
Charged Coupled Devices (CCD) are devices for the movement of electric charges. Together with silicon drift chambers they are called fully depleted pn CCDs and are able to detected particles and especially x-rays. The advantages are an enhanded sensitivity, an uniform responce and high speed of operation.
Strip Detectors usually have a n-type silicon bulk, a n^+-type backplane, where the positive bias voltage will be applied and p^+-type strip implants. The higher doping leads to a faster collection of the signal. The trips are covered with a silicon dioxide layer to prevent current directly draining into the delicate readout electronics. The thickness of the whole sensor is usually 300 µm. Future silicon sensors will have p-type silicon bulk and n^+-type strips. One of the advantage of this configuration is that the sensors can be operated even if they are not fully depleted. *Double Sided* Strip Detectors have instead of the n^+-type backplane strips, that are turned 90° compared to the other strips. The allows a 2D information, but they are more complicated to produce since both sides need to be processed.
Pixel Detectors are the most advantageous ones, since they provide 3D informations. They are build out of a 2D matrix of diodes, where each pixel gets its own readout chip. The common technology is the hybrid design, where pixel and readout electronics are produced seperatly and bump bonded together. The disadvantage are that Pixel detectors are expensive and produce a large data volumen. For this reason there are usually just used in the most inner parts of detectors.

3 The Wu Experiment [4]

The Wu experiment was the first experiment that proved a maximum parity violation in the weak β decay. It was the first confirmation towards the chiral nature of the weak interaction.

3.1 Historical Context

The parity $\hat{P}$ operator transforms a phenomen into its mirror image. A phenomen that is not identical to its mirror image is called chiral. Measurements of electromagnetic and strong interaction showed invariance under parity. As a result it was accepted that the mirror image of any physical process shows the same physics. In 1956 physicists believed that a system is invariant under the combination (CPT theorem) of parity $\hat{P}$, charge conjugation $\hat{C}$ and time reversal $\hat{T}$ as well as under each operation itself. In 1953 R.H. Dalitz adressed the so called $\tau - \theta$-puzzle which decribes the decay of two charged strange mesons:

$$\tau^+ = \pi^+\pi^+\pi^- \qquad \hat{P}\,|\tau\rangle = -1\,|\tau\rangle$$
$$\theta^+ = \pi^+\pi^0 \qquad \hat{P}\,|\theta\rangle = +1\,|\theta\rangle$$

Both particles have the same spin, charge, mass and lifetime, but different parity eigenvalues. Due to the principle of parity conservation this indicates that these are still to different particles. 1956 Lee and Yang proposed that τ and θ could be the same particle if the weak interaction violates parity conservation. They reviewed previous measurements and could not find any that ruled out the possibility of a chiral weak interaction. Hence they proposed that experimental states are a misture of states with usual and opposite parity. This leads to coupling constants C for parity conserving and $C^{'}$ for nonconserving interactions as well as $CC^{'}$ interference terms. It was not possible to distinguish between C and $C^{'}$ since the neutrino spin was not known back at the time. The misture has an effect on the angular distribution of nuclear interactions:

$$I(\vartheta)\mathrm{d}\vartheta \propto (1 + \alpha\cos\vartheta)\sin\vartheta\mathrm{d}\theta$$

where α is the asymmetry coefficient that contains the interference terms with $CC^{'}$. Lee and Yang proposed numerous possibilities to study the parity conservation of the weak interaction e.g. the angular distribution between an electron and a nucleus of a β decay.

3.2 Experimental Setup

The Wu experiment was carried out at the National Bureau of Standards (NBS) in Washington, D.C., by Chien-Shieung Wu and her low temperature group in 1956. They used the suggested β decay of a nucleus to verify if the weak interaction is chiral or not. The underlying principle was that changing the direction of the nucleus polarization is equivalent to a parity transformation.
One of the main challenges was the selection of the right nucleus for the experiment. They used ^{60}Co nuclei, because the corresponding β decay is a Gamow-Telller transition, where the emitted particles have a parallel spin. This is necessary to determine the chiral nature of the weak interaction.

$$^{60}Co \rightarrow\ ^{60}Ni^* + e^- + \bar{\nu}_e$$
$$^{60}Ni^* \rightarrow\ ^{60}Ni + 2\,\gamma$$

The second benefit is that the photons are emitted in the direction of the nucleus polarization. Therefore measuring the emitted photons allows to determine the polarization degree of the ^{60}Co nuclei. Two NaI scintillator are placed in a polar and equatorial position to the specimen to measure

the photons. The specimen is placed inside of a cryostat with a anthracene crystal at the top end to detected the β particles and emit photons which are then counted with a photomultiplier at the end of a Lucite light pipe. The photomultiplier is sensitiv to a specific energy corresponding to the energy of the β particle. Since the magnet moment of the electron is much greater as the one of the nucleus, a temperature close to absolute zero is necessary to polarize the nucleus. This method is called Gorter-Rose method and uses the principle of adaibatic demagnetization. The applied magnetic field reduces the entropy of the magnetic moments, afterwards the specimen is isolated adiabaticly and the magnet switched off. The present entropy of the system corresponds to a much lower temperature, which leads to instant cooling of the specimen. The used cerium magnesium nitrate bas a high anisotropic Landé g-factor ($g_1 \ll g_2$). This allows to apply a high magnetic field along g_1 with the first magnet and cool the salt down to around 0.003 K. Afterwards a solinoid is used to polarize the salt in direction of the second g-factor. The polarization of the orbital electrons enhance the magnetic field close to the nucleus. To use this effect a thin layer of ^{60}Co is vaporised on a CeMg nitrate crystal which together builds the specimen.

3.3 Results

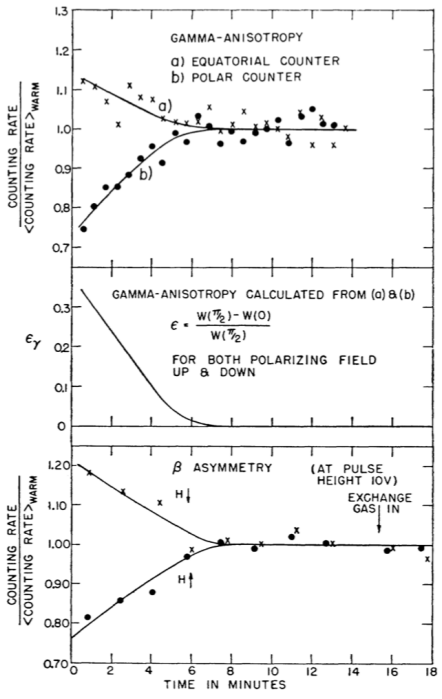

Figure 4: Gamma anisotropy and beta asymmetry for polarizing field pointing in positive and negative z direction. [4]

The spins of the neutrinos and electrons point in the same direction as the spin of the mother core due angular momentum conservation. Due to the polarization of the nuclei the spin direction is parallel to the magnetic field. Reversing the polarization of the magnetic field is identical to a parity transformation. The quantity of the emitted electrons was measured in negative z direction for both polarizations of the magnetic field. If parity is conserved the same amount of electrons will be emitted parallel and antiparallel to the nucleus spin. Therefore the same amount of electrons should be measured for both magnetic field configurations. The top and the bottom diagram in figure 4 are normalized with the counting rate of the warm setup, when the nuclei are not polarized. The top diagram shows the gamma anisotropy for the equatorial and the polar counter. It clearly shows that the polar counter is count less events compared to the warm configuration. From this rates are used to calculate the gamma anisotropy that is shown in the middle diagram. At the beginning a anisotropy of around 40 % is seen, which corresponds to a polarization degree of 60 % for the cobald nuclei. After around 6 min the setup is back to the unpolarized configuration. The bottom diagram final shows the β asymmetry for both magnetic field configuration. For the downwards direction the counting rate is exactly the same amount higher than the amount missing for the upward field direction. Furthermore the curse of the data point fits exactly the curse of the gamma anisotropy. This leads to the conclusion that the parity conservation is not only violated, but at a maximum.

Around the same time the Columbia experiment studied the angular destribution of a pion beam decaying weakly into muons, which then decay into electrons. They carried it out under the assumption that the muon is highly polarized if parity conservation is violated. They used a solinoid to change the orientation of the polarized muons and observed as well a large asymmetry corresponding to the changing field. Which shows again that parity conservation is violated.

4 The Goldhaber Experiment [5]

The Goldhaber experiment was the first one revealing that the neutrino is left-handed. It was an important step to confirm the chiral nature of the weak interaction.

4.1 Theoretical principles

The neutrinos are uncharged, colourless leptons, that exclusively interact weakly. Back in 1957 it was believed that neutrinos are massless. For massless particles the helicity is a lorentz invaraint quantity. As a consequence the helicity is identically to the chirality for the neutrino. So the neutrino is either left-handed or a right-handed particle. Left-handed is a particle where the direction of the spin is antiparallel to the direction of the momentum, for right-handed particles they are parallel. The Wu experiment delivered the first hint that the neutrino might be left-handed.
The main idea was to determine the neutrino helicity by using the conservation of angular distribution. When ^{152m}Eu captures an electron it decays into an neutrino and an excited $^{152}Sm^*$, which migrates into its ground state by sending out a photon with the energy of $E_\gamma = 960\,\mathrm{keV}$. Since the ^{152m}Eu is spin zero, the spin of the electron and the neutrino point in opposite directions. This is just possible for spin conservation if the excited Samarium state has the same spin direction as the electron. The recoil of the decay leads to roughly opposite momentum directions of the excited Samarium state and the neutrino. So the helicity of the neutrino and the excited Samarium is identical. Since the ^{152}Sm ground state is zero the helicity of the photon needs to be identically to the electron $H(\gamma) = H(e^-)$.

$$\overset{\Leftarrow}{{}^{152m}\mathrm{Eu}} + \overset{\Leftarrow}{\mathrm{e}^-} \longrightarrow \underset{\Leftarrow}{\overset{\Rightarrow}{\nu_\mathrm{e}}} + \underset{\rightarrow}{\overset{\Leftarrow}{{}^{152}\mathrm{Sm}^*}} \longrightarrow \underset{\Leftarrow}{\overset{\Rightarrow}{\nu_\mathrm{e}}} + \underset{\rightarrow}{\overset{\Leftarrow}{\gamma}} + {}^{152}\mathrm{Sm}$$

4.2 Experimental setup

The ^{152m}Eu was produced at a reactor at the Brookhaven National Labortory by bombarding europium oxide with neutrons. The time for the experiment was limited by the halflife time of the ^{152m}Eu with $T_{1/2} = 9.3\,\mathrm{h}$. The two main tasks to determine the neutrino helicity was determine the neutrino flight direction and measure the photon polarization.
The neutrino flight direction can just be measured indirectly with the method of resonant scattering fluorescence. The neutrino and the excited Samarium are emitted back to back but in random direction. Since the photon is emitted with a fixed energy it is able to again excite another Samarium nucleus in a target. By doing to the the flight direction of the corresponding neutrino is fixed. The problem is that energy loss $E_\mathrm{loss} \approx 6\,\mathrm{eV}$ due to the recoil momentum at the emission and absorption of the electron is two orders of magnitude larger than the line width of the ^{152}Sm target.

$$E_\mathrm{recoil} = \frac{E_\gamma^2}{2M_{^{152}Sm}c^2} \approx 3\,\mathrm{eV}$$

The resonant scattering is only possible if the Doppler shift has a size of $\approx 6\,\mathrm{eV}$. At room temperature $T \approx 300\,\mathrm{K}$ the mean velocity of the atoms lead to a Doppler shift of around $0.5\,\mathrm{eV}$, if the the Samarium ground state and the photon move back to back. So the thermal Doppler shift is not enough, but together with the Doppler shift from the neutrino recoil, considering a neutrino energy of $E_\nu \approx 940\,\mathrm{eV}$, is is.

$$\Delta E_\mathrm{thermal} = E^2\sqrt{\frac{2k_BT}{M_{^{152}Sm}c^2}}\cos\vartheta \approx \cos\vartheta 0.5\,\mathrm{eV}$$

$$\Delta E_\mathrm{neutr} = \frac{EE_\nu}{M_{^{152}Sm}c^2}\cos\vartheta \approx \cos\vartheta 5.4\,\mathrm{eV}$$

The measurement of the photon polarization was based on the fact that $H(e^-) = H(^{152}Sm^*) = H(\gamma)$. A iron housing is placed around the ^{152m}Eu and then magnetized, which forces most of the electrons in the iron to align antiparallel to the magnetic field. Since the compton cross section is greater for the left-handed photons, they are more likely to pass trough the iron.
The reminding right-handed photons can be neglect, since they need to flip the electron spin to pass trough the iron. This leads to an energy loss that is too great for the photon to still be able to excite the ^{152}Sm target.

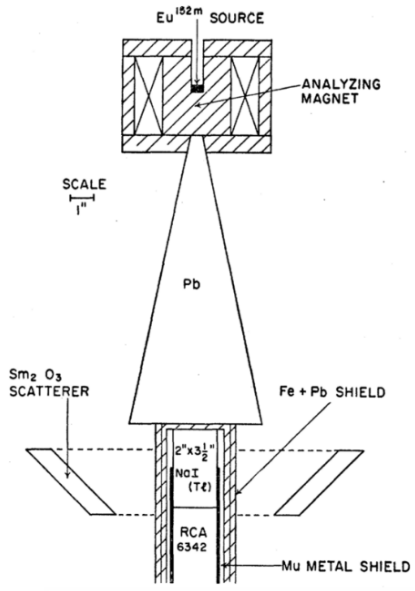

Figure 5: Schematic representation of the Goldhaber experiment.[5]

Combining both principles lead to the possibility to determine the neutrino helicity. As figure 5 shows the ^{152m}Eu source is embedded in the magnet and on top of a lead shield. Below the shielding the NaI scinitillator is placed in the middle of a Samarium ring, which is used to detect the resonant scattering photons. The shielding should protect the scinitillator against radiation from the Europium itself. It is also placed inside of an iron box to protected it from the magnetic field.

4.3 Results

The photon scattering spectrum gets measured every 3 minutes and afterwards the magnetization gets flipped. Nine measurements have been beformed in total and lead to an estimated, average photon polarization of 0.67 ± 0.10. This was in good agreement with the theoretical prediction of 0.84. The counting rates in the photopeaks have been compared for the magnetic field pointing up N_+ and down N_-. It lead to an effect of

$$\delta = 2 \cdot \frac{N_- - N_+}{N_- + N_+} = 0.017 \pm 0.003 \, .$$

This proves that more gamma rays have been observed with the magnetic field pointing downwards. Which means that only left-handed photons transmit and gives the final result:

$$H(\nu) = -1.0 \pm 0.2 \, .$$

This was considered as the evidence that the neutrino in a β decay is 100 % left-handed. Till today only left-handed currents for particles and right-handed currents for antiparticles have been observed. This result did not changed with the discovery of the neutrino masses, since they are so small. But it could not be ruled out completely if there is not an admixture of righthandedness. Till today it is unkown if the neutrino is a dirac or a majorana particle, which means if it is its own antiparticle. Searches for neutrinoless double β decay try to determine the ν nature.

5 Discovery of Neutral Currents [6]

The neutral currents were discovered with a neutrino beam at the bubble chamber Gargamelle. It was the first experimental proof of the theory for the electroweak unification and lead to the acceptance to describe the standard model with quantum field theories.

5.1 Theoretical principles

Till the begining of the 1930 the β decay $n \to p + e^-$ was under as a two body decay. In this case angular momentum conservation is violated and it was not possible to explain the experimentally observed continuously energy spectrum of the electron. The solution to this problem was given by W. Pauli in 1930. He postulated a at the time unkown, uncharged and extremly light particle with a half numbered spin. This particle is today known as a neutrino and concludes the β decay. In 1933 introduced E. Fermi the classical theory of the weak interaction. It was described by a point interaction of four fermions. The theory is just valid for the low energy limes, since it is not renormalizable.
The V-A structure of the weak interaction was first proposed in 1948 by Feynman and Gell-Mann as well as Marshal and Sudarshan. After the parity violation was shown by the Wu experiment, more investigations took place to understand the nature of the weak interaction. In 1968 the so called Glashow-Salam-Weinberg (GSW) model was proposed, which described the electroweak unification $SU(2)_L \times U(1)_Y$. Since the weak interaction, with the $W_\pm$, violates the parity conservation but the electromagnetic interaction conservers it a forth boson was needed. The Higgs mechanism broke the electroweak symmetry, as a result one of the weak and the hypercharge bosons mix to the two physical bosons Z^0 and γ. In addition the $W^\pm$ and the Z^0 boson get mass induced, while the photon γ remains massless.
The prediction of the Z boson immediately leads to the existence of neutral currents. The in 1963 introduced Cabibbo angle explained the difference between weak eigenstates and mass eigenstates. This theory allowed flavour changing neutral currents (FCNC), but experimental results showed that they are strongly suppressed. The solution was given by the GIM mechanism in 1970. The proposal of an additional charm c quark lead to the result that FCNC are suppressed due to the Z^0 boson.
The search for neutral currents was not a priority of the experiments by the time. This changed in 1971 as G. 't Hooft proved that the GSW model is renormalizable.

5.2 Experimental setup

The Gargamelle experiment was the biggest one at the time. The advantage of this is that the long pathlength of entering particles make it possible to distingluish muons and pions and study the hadronic decay of the neutron. The exponentiel absorption of the neutrons fits completely into the chamber, which gives the possibility to study the course as well as the angular distribution. This was later very imporant to study the neutron background of the neutral current events. The basic principle of a bubble chamber is that a liquid enters a metastable phase by heating it below its boiling point and decreasing the preasure afterwards. If a charged particle now hits the chamber it leaves a ionisation track which leads to bubbles that can be photographed. Usually a magnetic field sourronds the chamber to bend the particle tracks. This allows to determine the momentum. The Gargamelle chamber had a volume of $V = 12\,\mathrm{m}$ and a magnetic field of $B = 2\,\mathrm{T}$. The used liquid was Freon. To provide the neutrino beam a proton beam with a center of mass energy of $\sqrt{s} = 26\,\mathrm{GeV}$ was extracted at CERNs Proton Synchrotron (PS) and adjust onto a berylium target. By this kaons and pions get produced which will be focused through a magnetic horn and afterwards decay weakly in the 70 m long decay tunnel. In front of the bubble chamber is a iron shielding so just the neutrinos can enter the chamber. To determine the neutrino flux the muon flux was measured since they are propotional.

5.3 Measurement and results

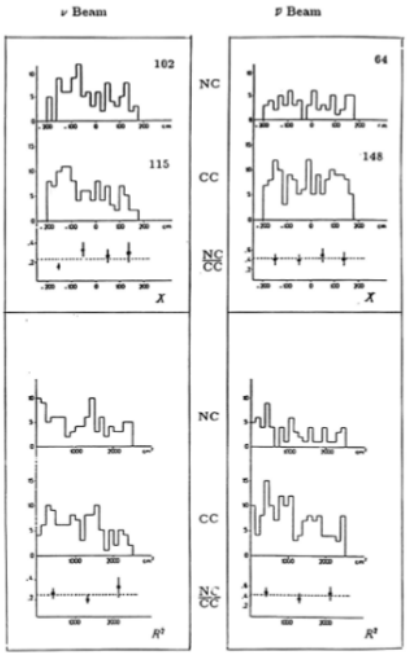

Figure 6: Longitudinal and radial distribution of neurtral current and charged current events.[6]

The typical measurement of an energy distribution was not possible since it was not known how much energy the neutrino carries. It was solve my measuring the rate $R = \frac{NC}{CC}$ of the neutral currents compared to the charged current events.
The process associated with the charged current is $n + \nu_\mu \rightarrow p + \mu^-$ and with the neutral current $p + \nu_\mu \rightarrow p + \nu_\mu$. Figure 6 shows the counted events that are associated with neutral currents and charged currents. The left side shows the results for the ν beam and the right for the $\bar{\nu}$ beam. The top diagrams correspond to the longitudinal and the bottom ones to the radial position. For both confirgurations the ratio is significant different from zero. The next step was to study the background in detail. It is mainly evoked to neutrons entering the chamber, that a the result of hadronic cascades in the shielding. Figure 7 shows possible tracks of neutral current (NC), charged current (CC) and the associated (AS) neutron events.
As mentioned before the bubble chamber is long enough to study several properties of the neutrons, this allows to predict the energy distributions of the neutral current events and the associated neutron events. The peaks of the distributions are at different points, so the energy cutoff of $E > 1\,\mathrm{GeV}$ reduces the neutron background a little bit. But in general there are two different types of neutron events. The AS events are neutrons produced inside of the chamber, but there are also background (B) events that contain neutrons produced in the shielding [7].
Together they form the total neutron background and can be calculated with

$$N_{\mathrm{ges}} = B + AS \qquad\qquad \frac{B}{AS} = \frac{1}{\left\langle 1 - \exp\left(\frac{-L}{\lambda}\right)\right\rangle - 1}\ .$$

L is the distance to the end of the downstream and λ is the measured, characteristic interaction length. Both quantities have been measured and the final result was that around 20 % of the measured NC events where actually neutron events. Since the physics did not trust there results after a few false discoveries in the past, they applied really strict selection criteria. They include applying the high energy cut, charged events that have the possibility to not be a muon, possible cosmic events or particles that possible entered the chamber together with the beam got rejected. As well as so called μ-kink events, which are muon like events with a suddenly vanishing muon track. This is a sign that it actually was a pion or proton. The final ratio combining the results of the ν and $\bar{\nu}$ beam was

$$R = 0.28 \pm 0.03$$

This leads to the conclution that the NC events are not dominated by neutron events and neutral currents have indeed been observed. It was the first confirmation of the GSW model and lead to the nobel prize in 1979.

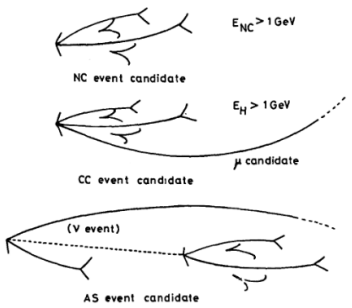

Figure 7: Schematic representation of the tracks in the chamber. There are neutral current, charged current and associated events. [7]

6 The Discovery of CP violation [8]

The CP asymmetry was discovered in the kaon sector at the Finch experiment in 1964. And was in important step towards the understanding of the weak interaction. The origin of the CP violation was explained in the CKM matrix assuming that three or more quark generations exist.

6.1 Theoretical principles

In the years prior to the discovery of CP violation, parity and charge conjugation violations due to the weak interaction were observed, but there was no evidence of CP violation. At this time were just three quarks known the u, d and s. Only in 1964 the $c$quark was postulated to explain the suppression of FCNC. The mass eigenstates K^0 and $\bar{K}^0$ have the same CP eigenvalue. This lead to the conclution that the CP eigenstates are a linear combination of both mass eigenstates:

$$|K_1\rangle = \frac{1}{\sqrt{2}}\left(\left|K^0\right\rangle + \left|\bar{K}^0\right\rangle\right)$$
$$|K_2\rangle = \frac{1}{\sqrt{2}}\left(\left|K^0\right\rangle - \left|\bar{K}^0\right\rangle\right)$$

To conserve the CP symmetry K_1 can only decay into two pions, while K_2 decays into three pions. Since the decay into three pions needs more phase space, the lifetime of the K_2 is longer as the one of the K_1. This is the reason for the identifictaion $K_L = K_2$ (L=long) and $K_S = K_1$ (S=short). The mesons K^0 and $\bar{K}^0$ also interact different with matter. While the K^0 mainly contributes to scattering processes, the $\bar{K}^0$ produces additional excitations of hyperons. This reason leads to a higher cross section and is the reason, that a part of the K_L transitions to K_S. This was the idea for the measurment of the Finch experiment and would prove the CP violation in weak interactions.

6.2 The Cronin-Fitch Experiment

The Cronin-Fitch experiment took place at the Brookhaven National Labratory. The idea was to place the detector far away from the interaction point, so all reminding Kaons are K_L. If then a decay into two pions would have been observed, that would be a measurement of indirect CP violation.
The experiment is assambled out of a two-armed spectrometer and a helium bag to reduce possible interactions. The spectrometer arms contain a spark-chamber before and behind a magnet and use a scintillator together with a water Cherenkov counter as a trigger. The principle of the measurement was to measure the angle ϑ, where the sum of the momenta comes together. The second idea is to check that deposited energy is around the kaon mass. They observed a peak at $\cos(\vartheta) = 1$ compared to the Monte Carlo data. This lead to the branching $BR(K_L^0 \to \pi^+\pi^-) = (2.0 \pm 0.4) \cdot 10^{-3}$. This is a clear observation of a two-body decay of K_L and proves CP violation. The actual CP eigenstates are

$$|K_S\rangle = \frac{1}{\sqrt{1+|\epsilon|^2}}(|K_1\rangle - \epsilon\,|K_2\rangle)$$
$$|K_L\rangle = \frac{1}{\sqrt{1+|\epsilon|^2}}(|K_2\rangle + \epsilon\,|K_1\rangle)\,.$$

that allow a indirect measurement of the CP violation with $\epsilon = (2.228 \pm 0.011) \cdot 10^{-3}$. A direct observation of CP violation by proving that $\Gamma(K_0 \to \pi\pi) \neq \Gamma(\bar{K}_0 \to \pi\pi)$ was done by NA48 at CERN and KTeV at Fermilab in 1999. The third type of CP violation oigins from the interference between mixing and decay. The corresponding eigenstates are $|M_L\rangle$ and $|M_H\rangle$ corresponding to states with a **l**ow and **h**igh mass. $|M_{L/H}\rangle = p\,|M_0\rangle \pm q\,|\bar{M}_H\rangle$ with $|p|^2 + |q|^2 = 1$. This eigenstates play a significant role for B mesons.

6.3 CKM Matrix and the B meson sector

In 1963 Cabibbo postulated a matrix, which could describe the mixing ot two quarks. In 1973 Kobayashi and Maskawa extended the matrix with a third quark generation. This lead to three mixing angles and a complex phase that could explain the CP violation. In the Standard Model quarks get their masses trough Yukawa interaction. The non-diagonal Yukawa matrices can be diagonalized with unitary matrices. This leads to a change into the flavour base. The problem is that the Yukawa matrices for up- and down-type quarks cannot be diagonalized together. The remaining component is the CKM matrix, which is a unitar matrix as well.
The experimental results for the mixing angles are $\vartheta_{13} \ll \vartheta_{23} \ll \vartheta_{12} \ll 1$. Since the complex phase only occurs with $\sin\vartheta_{13}$, the CP violation is highly suppressed. Because of the unitar nature of CKM matrix, there are different unitarity triangles that can be constructed from this condition. These can be measured precisely with B mesons, since they have lower hadronic uncertainties and a higher sensitivity for the unitary angles. The CKM matrix predicted a large asymmetry in $B\bar{B}$ oscillations. They were dominated from $m_t^2|V_{tb}V_{td}|^2$ contributions. In the 1990s they build the first B *factories* at e^+e^- collidern. In 2001 BABAR and BELLE confirmed the CP violation in the B sector.
CP violation was measured over the time difference between the B^0 and the $\bar{B}^0$ decay. The $B^0\bar{B}^0$ pair is produced highly boosted. One decay channel gets fully reconstructed and one is favour tagged, since the pair builds an entangled quantum state. The violation can be measured with the number of B^0 and $\bar{B}^0$ mesons decaying into a final, CP eigenstate f.

$$A_{CP}(f,t) = \frac{N(\bar{B}^0 \to f) - N(B^0 \to f)}{N(\bar{B}^0 \to f) + N(B^0 \to f)} = S_F \sin(\Delta m t) - C_F \cos(\Delta m t)$$

The prefactors S_F and C_F depend on the decay mode and can be used to determine the unitarity triangle. The combined results of all current measurements is shown in figure 8. Currently all

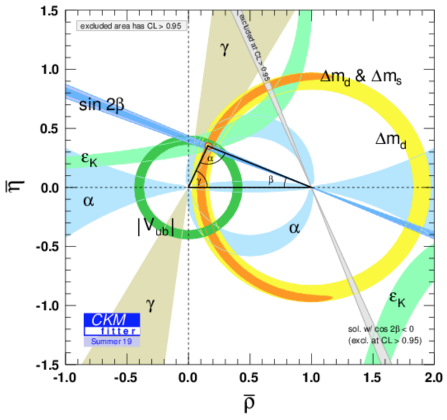

Figure 8: Global average for one unitary triangle. [8]

measurements are in agreement.
The Jarlskog invariant measures the strength of the CP violation:

$$J = 2A_\Delta = (3.060^{+0.071}_{-0.079}) \cdot 10^{-5} \tag{1}$$

Besides the observation of CP violation in $B^0\bar{B}^0$ systems, it was also possible to determine it in B_s and D systems.
Furture experiments aim for higher precisions in determining the different parameter of the unitarity trianle. Beside this there will be also studies for CP violation in the leptonic sector. Due to the small size of SM CP violation it is also not able to answer the question of the matter-antimatter asymmetry of our universe.

7 $B\bar{B}$ Oszillations [9]

For a long time the measurement of B oscillations was considered impossible. In 1986/87 measurements of the decay width of B mesons showed that it was smaller than expected and thus oscillations could be observed. In 1987 they finally have been discovered by the ARGUS experiment at DESY.

7.1 Theoretical principles

The 2dimensional Cabibbo matrix was the first attempt to describe the difference between mass and weak eigenstates in the quark sector. The CKM matrix was an expansion to this theory by considering at least three generation of quarks. The CKM matrix provides four indepenten parameters, three mixing angles and one complex phase. This phase is the origin of CP violation in weak interactions. Another form of representation for the CKM matrix is the Wolfenstein parameterization. The hierachy of the different entries is expressed by orders of $\lambda = \sin\vartheta_{12} \approx 0.22$.
The time evolution of unmixing mesons is given by the exponential decay law. For a mixing mesons the Schrödinger equation is extended to a two-dimensional equation system. The mass eigenstates B_L and B_H can be extracted by diagonalizing the system. The weak eigenstates B^0 and $\bar{B}^0$ are linear combinations of this mass eigenstates. Both mass eigenstates have different masses and indepentent decay width. For B mesons it is possible to use the approximation of nearly equal decay widths for both mass states. Therefore the weak eigenstates can be written as follows:

$$|B^0(t)\rangle = \frac{1}{2p}(|B_L(t)\rangle + |B_H(t)\rangle) \quad = \frac{e^{-\Gamma t/2}}{2}[(e^{-im_L t} + e^{-im_H t})\,|B^0\rangle + \frac{q}{p}(e^{-im_L t} - e^{-im_H t})\,|\bar{B}^0\rangle]$$
$$|\bar{B}^0(t)\rangle = \frac{1}{2q}(|B_L(t)\rangle - |B_H(t)\rangle) \quad = \frac{e^{-\Gamma t/2}}{2}[(e^{-im_L t} + e^{-im_H t})\,|\bar{B}^0\rangle + \frac{p}{q}(e^{-im_L t} - e^{-im_H t})\,|B^0\rangle]$$

Therefore the oscillation probabilites are given by:

$$P(B^0 \to B^0[\bar{B}^0]) = |\langle[\bar{B}^0]B^0|B^0\rangle|^2 = [\left|\frac{q}{p}\right|^2]\frac{e^{-\Gamma t}}{2}(1 \pm \cos(\Delta m t))$$

This leads to the conclusion that the CP asymmetry only depends on the mass difference of both states and the flight-time:

$$A_{CP} = \frac{P(B^0 \to B^0) - P(B^0 \to \bar{B}^0)}{P(B^0 \to B^0) + P(B^0 \to \bar{B}^0)} = \cos(\Delta m t)$$

The most common measurements of B mesons are performed with $B_d^0\bar{B}_d^0$ and $B_s^0\bar{B}_s^0$. This leads to $\Delta m_d \sim m_t^2|V_{tb}V_{td}|^2 \sim m_t^2\mathcal{O}(\lambda^6)$ and $\Delta m_s \sim m_t^2|V_{tb}V_{ts}|^2 \sim m_t^2\mathcal{O}(\lambda^4)$. Since $\Delta m_s \sim \frac{1}{\lambda^2}\Delta m_d$ oszillates the B_s^0 meson much faster than B_d^0.

7.2 ARGUS

The basic principle for the measurement of $B\bar{B}$ Oszillation is to produce the $\Upsilon(4s)$ resonances at e^+e^- collidern that decay approximate 50 % into $B\bar{B}$ pairs. Afterwards all events containing a B meson pair need to be reconstructed to determine the decay ratio $r = \frac{N(B^0B^0)+N(\bar{B}^0\bar{B}^0)}{N(B^0\bar{B}^0)}$. If $r > 0$ does $B\bar{B}$ oszillations exist. The considered decay of B mesons does involve D mesons, that then decay into K and π mesons.
The collision point of the ARGUS experiment was surrounded by a vertex chamber, followed by drift chambers and time of flight counters in front of shower counters. These were followed from solenoid coils and iron yokes in front of the muon chambers. In the direction of the beam pipe the vertex

chamber was followed by compensation coils in front of mini beta quadrupoles.
The mini beta quadrupoles were placed inside the detector to improve the luminosity. The compensation coils ensured that the magnetic fields of the quadrupoles did not interfered with the solenoid. If a charged particles traveled trough the drift chamber, it ionized the gas along its flight path. Together with the solenoid this provided a good momentum resolution. The time of flight counters were made out of scintillation counters. By measuring the flight time, they provided a possibility to determine the velocity of charged particles. Together with the momenta, it was possible to itentify particles over their rest mass.

7.3 Performed Measurement

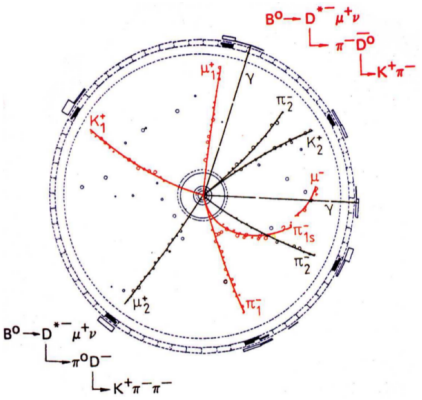

Figure 9: ARGUS event display of a B^0B^0 event.[9]

They used three different methods to reconstruct the events. The first method is a full event reconstruction, which has the smallest background. But the statistics are too small to determine r. The second method is to reconstruct semi leptonic decays, which leads to higher statistics, but misidentification of leptons and therefore of B mesons. Figure 9 shows a possible event display. Different backgrounds are e.g. continuum dilepton sources or lepton hadron misidentification. They get supressed with momentum and angle cuts as well as using informations from invariant masses to reject background events from resonance decays. The background analysis was also performed with data from well known decays to improve it.

$$r = \frac{[N(l^+l^+) + N(l^-l^-)(1+\lambda)]}{N(l^+l^-) - [N(l^+l^+) + N(l^-l^-)]\lambda} = 0.22 \pm 0.09 \pm 0.04$$

$$\text{with } \lambda = \frac{f^+}{f^0}\left(\frac{\text{Br}^+}{\text{Br}^0}\right)^2 = 1.2$$

The third method is a compromise between the first two, which reduces the background. This method fully reconstructs one B meson and the other one is tagged with a semi leptonic decay. The errors are bigger since the statistics are smaller.

$$r = \frac{N(B^0l^+) + N(\bar{B}^0l^-)}{N(B^0l^-) + N(\bar{B}^0l^+)} = 0.20 \pm 0.12$$

The combined result is $r = 0.21 \pm 0.08$ and is a clear evidence for $B\bar{B}$ oscillations.
The ratio is also proportional to the Δm, which allows to set a lower limit to the top quark mass of $m_t \geq 50\,\text{GeV}$.

The LHCb collaboration performed high preccision measurement of B_d^0 and B_s^0 meson oscillations. They determined the mass differneces to:

$$\Delta m_d = 0.5156 \pm 0.0051(\text{stat.}) \pm 0.0033(\text{syst.})/\text{ps}$$
$$\Delta m_s = 17.768 \pm 0.023(\text{stat.}) \pm 0.006(\text{syst.})/\text{ps}$$

8 The Discovery of the Gluon [10]

The gluon was discovered by the measurement of three jet events at the e^+e^- collider PETRA. It was the first confirmation of the quantum chromodynamic (QCD) and also the first discovered gauge boson after the photon.

8.1 Historical Context

Around 1954 the developement of the QCD and the Yang-Mills theory started. Together, both theories build the foundament, which leads to the formulation of the gauge theories of the weak and strong interaction. In 1964 Murray Gell-Mann and George Zweig brought up the quark hypothesis. It was the first time that quarks were mentioned as components of hadrons. But at this point, it was still unclear which force binds the quarks into hadrons and if quarks could also be free. If this force is caused by a new interaction there would also be the possibility of having a new exchange particle. Beside this idea there was the experimental evidence that the wavefuntion of the fermion Δ^{++} is symmetric under the exchange of two quarks. This was in disagreement with the Pauli principle which suggests that fermion wavefuntions need to be antisymmetric. Oscar W. Greenberg fixed that problem by postulating another quantum number, **Colour**, in 1964. The colour could uppear in three different states *red*, *blue*, *green* and their anti versions. Together with the colour wavefuntion the total wavefunction of the baryon was again antisymmetric. An experimental indication for this three colours was given by the ration between the cross section of e^-e^+ into two quarks and two muons. The experimental results showed missing factor of 3 in the theoretical prediction. The results from electron-proton scattering at the Standfort Linear Accelerator Center (SLAC) indicated that just 50 % of the total proton momentum were carried by quarks. This interpretation was done by Chris Llewellyn-Smith in 1968 and was the first indication for the gluon. In 1973 David Politzer, David Gross and Frank Wilczek formulated the QCD as a $\mathrm{SU}(3)_{\mathrm{colour}}$ group with the gluon as gauge boson corresponding to the interaction. In 1975 the e^-e^+ collider SPEAR at SLAC provided the first measurements of two jet events ($e^-e^+ \to q\bar{q}$). In the following year John Ellis, Graham Ross and Mary Garllard formulated the possibility of gluon production trough bremsstrahlung. This process would lead to corrections for the two jet events at higher energies.
In 1979 the oberservation of three jet events from the TASSO collaboration at the PETRA collider at the Deutsches Elektron-Synchrotron (DESY) finally lead to the discovery of the gluon.

8.2 Theoretical principles

The QCD is a relativistic quantum field theory and describes the strong interaction. It is based on the $SU(3)_{\mathrm{C}}$ symmetry group, which leads to eight generators, the gluons. They are the gauge bosons of the QCD and mediate the strong force. Analog to the electric charge of the quantum electrodynamic the corresponding charge of the QCD is the colour. Therefore the massless gluons couple to the colour charge of particles. Since the $SU(3)_{\mathrm{C}}$ is non-abelian the gluons carry colour themselves and therefore interact with each other. The gluons are vector bosons and therefore the spin is 1.
The QCD has two important characteristics emerging from the fact that the coupling constant $\alpha_S(q)$ is running. In the case of small distances between coloured particles or high momentum transfer they become asymtotically free. This phenomen is called asympotic freedom and gives an explanation why there is a lower energy limit for gluon bremsstrahlung. The second characteristic of the strong interaction is the colour confinement. After a specific distance between two colour charged particles it is energetic favoured two produce two new particles between the initial ones. This is caused by the high value of the coupling constant at long distance. The confinement is the reason that in nature just colour neutral, white, states exist. They are bounded stated of colour charged particles. More important for high energy physics is that the confiment leads to hadronization. It leads to the

production of several new particles due to high energetic scattering processes. This is the reason why the initialy produced quarks will be measured as jets. The sum over the momenta of all hadrons is equal to the momentum of the initial quark.

8.3 Experimental Setup

The Deutsche Elektonen.Synchroton (DESY) was founded at the 18.12.1959 in Hamburg. In 1974 was proposed to build the Positron-Elektron-Tandem-Ring-Anlage (PETRA). PETRA was completed in October 1978 and with a perimeter of 2.3 km the biggest storage ring at a time. It operated at a center of mass energy between 13.7 GeV to 27.4 GeV. The ring include four interaction points where the five collaborations TASSO, JADE, MARK J, CELLO and PLUTO worked. TASSO succeeded in discovering the gluon by measuring three jet events in 1979. TASSO was a **T**wo **A**rm **S**pectrometer **SO**lenoid detector. A scintillation counter, proportional chamber and a large drift chamber allowed to measure charged particles. The surrounding solinoid helped to measure the momenta more precisely. The two arms contained Cherenkov detectors and time of flight counters, which made it possible to distinguish between pions, kaons and protons.

8.4 Measurments that lead to the Discovery

By the time that the idea of gluon bremsstrahlung was developed, experiments start to search for events that indicate this type of bremsstrahlung. If such events exist the three jets lie in an event plane which is spanned by the three momentum vector of the initial quarks and the gluon. Sau Lan Wu made the pediction that such events would appeare at center of mass energies greater then 22 GeV. In June 1979 the TASSO collaboration presented several three-jet events. But before calling it the discovery of the gluon they started to analyse their data more detailed.

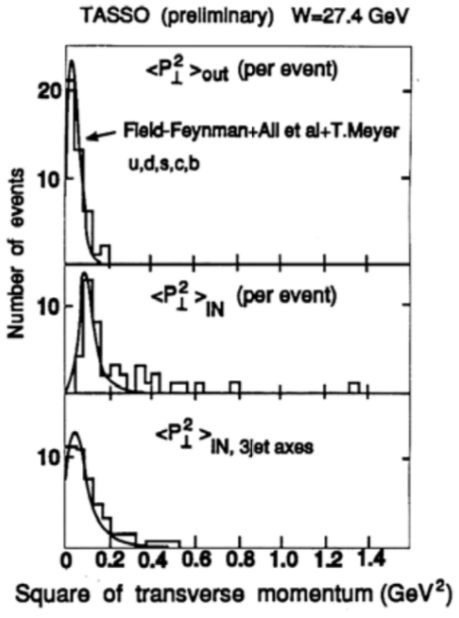

Figure 10: Comparising of $\langle p_T^2 \rangle_{\text{out}}$ and $\langle p_T^2 \rangle_{\text{in}}$ with the $q\bar{q}$ and the $q\bar{q}g$ model.[10]

The third jet has to come from a boson, so the first cross check made, was if it is possiple that a meson could produce such a jet. This is not possible for a quark to emit a meson with such large momentum at the present rate. The TASSO collaboration made different measurements at energies below and above the neccessary center of mass energy to produce gluon bremsstrahlung. This made it possible to study the energy dependent kinematics. In partically two different $< p_T >$ analysis haven been performed. Therefore a jet axis is fitted to the final state momentum of each hadronic event. In the case of $q\bar{q}$ jet production without a gluon the two jets would have the same momentum but in opposite directions. Due to this fact the contributions should cancel each other to zero in $< p_T^2 >$. The energy time uncertainty causes a $< p_T^2 >$ value slightly different from zero, but it is still independent from the center of mass energy. In the case of the presence of another particle the momenta would not cancel each other anymore and a asymmetry would be observed. The asymmetry would rise with higher energies. The measurements made by the TASSO collaboration indicated the last case. Other measurement at the time helped to rule out that the third jet could come from a heavier quark. The second study already used the idea of having three jets that create an event plane. The conservation of energy and momentum allows to define two quantities $\langle p_T^2 \rangle_{\text{out}}$ and $\langle p_T^2 \rangle_{\text{in}}$ to characterise, how planar the event plane is. $\langle p_T^2 \rangle_{\text{out}}$ is

the mean squared transverse momentum normal to the plane and $\langle p_T^2 \rangle_{\text{in}}$ the mean squared transverse momentum in the plane. For the case of $\langle p_T^2 \rangle_{\text{out}}$ the $q\bar{q}$ model fits the data pretty well, this is also the case for $\langle p_T^2 \rangle_{\text{in}}$ at low energies. But but for higher energies there appeare events in the event plane, while the model does not predict them. In particular is one event for $\langle p_T^2 \rangle_{\text{in}} > 0.3\,\text{GeV}$ predicted and eleven where observed. The data fit the model of a three jet event. Based on this result the possibility of three jets as a result of statistical fluctuation of the process $e^- e^+ \to q\bar{q}$ could be ruled out. Taking all this results into account this was indeed the discovery of the gluon. The discovery was confirmed by the other experiments within the following two month.
As a follow up the TASSO collaboration studied the spin of the gluon, to find out if the gluon is a vector boson as predicted. John Ellis and Inga Karliner predicted that the cross section depends on the so called Ellis Karliner angle. Depending on the spin of the gluon the shape of the distribution is significant different, if the gluon is a vector boson or a scalar. The measurement showed a clear agreement with the vector boson distribution. The discovery of the gluon and the oberservation that it is indeed a vector boson lead to the confirmation of the quantum chromodynamic.

9 The Discovery of the W and Z Bosons [11]

9.1 Theoretical principles

In the 1960s Glashow, Salam and Weinberg proposed the electroweak theory $SU(2)_L \times U(1)_Y$. They used the Higgs mechanism to spontanously break the electroweak symmetry into the $U(1)_{em}$. The mass eigenstates after the spontanous symmetry breaking (SSB) are a linear combination of the gauge eigenstates, B, W^1, W^2 and W^3, and a rotation with the Weinberg angle ϑ_W. They also lead to the mass predictions:

$$\gamma = W^3 \sin\vartheta_W + B\cos\vartheta_W \qquad m_\gamma = 0$$
$$Z^0 = W^3 \sin\vartheta_W - B\cos\vartheta_W \qquad m_Z = \frac{m_W}{\cos\vartheta_W} = (80 \pm 25)\text{GeV}$$
$$W^\pm = \frac{1}{\sqrt{2}}(W^1 \pm iW^2) \qquad m_W = \sqrt{\frac{\pi\alpha}{\sqrt{2}G_F}}\frac{1}{\sin\vartheta_W} = (68 \pm 40)\text{GeV}$$

The high mass of the weak gauge bosons is the reason that the weak interaction is short ranged. The bosons couple through the conserved weak isospin, which includes all SM particles beside gluons.
Till 1975 the weak force was known from radioactive beta and muon decays as well as the discovery of neutral currents. Experimentelle evidence for the weak gauge bosons was still missing. Till the $W^\pm$ and the Z^0 decay both in hadronic and leptonic final states, the searches were focused on the much cleaner leptonic decays. The only possibility to discover the W boson at lepton colliders was due to pair production which requieres a centor of mass energy of at least $\sqrt{s} \approx 140\,\text{GeV}$. To reach this energies was not realizable with the technology back at the time. This is why the searches were executed at hadron colliders. The boson masses could be reconstructed from the final states with $q\bar{q} \to W^+ \to l^+\nu_l$ and $q\bar{q} \to Z^0 \to l^+l^-$. Since in the 1970s there was a little known about parton distribution functions, the easiest way to make sure that enough antiquarks were present was due $p\bar{p}$ collisions.

9.2 Experimental Setup

C.Rubbia, P. McIntyre and D.Cline proposed this possibility to search for massive neutral intermediate vector bosons in 1976. Since CERN already planned LEP, they focused to propose an upgrade of the Super Proton Synchroton (SpS) to a center of mass energy of $\sqrt{s} \approx 400 - 800$ GeV and the use $p\bar{p}$. In 1981 the measurments with the new SppS started.
Since the branching fraction of the Z boson into two charged leptons at $\sqrt{s} = 600\,\text{GeV}$ is so small, $3 \cdot 10^{10}$ antiprotons are needed per day to create one of the requiered events. This rate can be achiebed by firing the Proton Synchroton beam at a target and extracting the antiprotons. The problem is that the antiprotons occupy a too large phase space volume. S. van der Meer invented the process of stochastic cooling to increase the phase space density in 1972. Particles that deviate from their ideal path are registered by an electrode. The signal of this electrode is transmitted to a kicker magnet to bring the particle back to its desired orbit. After this technology was successfully tested, the upgrade of the Sps to the SppS was approved in 1978.
The Underground Area 1 experiment (UA1) was the first general-purpuse detector that almost all of the solid angle. The problem is that they used a dipol magnet which lead to false discoveries like monojets. The second experiment (UA2) had to be cheaper and therefore missed a central magnet and muon chambers. They concentrated on the calorimeter to optimize it for the detection of electrons. Both experiments were used to verify the results of each other.

9.3 Measurements

Both experiments searched for the decay $W^{\pm} \rightarrow \ e^{\pm} + \overset{(-)}{\nu}_e$. They had to reconstruct the missing transverse momenta $\vec{p}_{\mathrm{T}}^{\,\mathrm{miss}}$ to take advantage of the involved neutrino. The following applies to the transverse pulses $\sum_{\mathrm{cells}} \vec{p}_{\mathrm{T}} = 0$ in the case of a perfect measurement. Therefore the missing transverse momentum is equivaltent to $\vec{p}_{\mathrm{T}}^{\,\mathrm{miss}} = \sum_{\mathrm{cells}} \vec{p}_{\mathrm{T}}$.
The data for the W boson search were taken at a 30-day run and delivered approximate 2000 triggered events. Both collaborations searched for one isolated charged track that deploys $E_{\mathrm{T}} > 15\,\mathrm{GeV}$ in an electromagnetic cluster. UA1 required an energy deposit below 600 GeV in the hadronic calorimeter and UA2 checked if the shower topology matches the expactation for an isolated electron along the track. This led to 39 UA1 events and 4 UA2 events. Events with high transverse momentum electrons seemed to be correlated to high missing transverse momenta events. Further cuts were applied to access the significance if correlation. The UA1 requiered a $\vec{p}_{\mathrm{T}}^{\,\mathrm{miss}} > 15\,\mathrm{GeV}$ together with $E_{\mathrm{T}} > 15\,\mathrm{GeV}$ and UA2 $\vec{p}_{\mathrm{T}}^{\,\mathrm{miss}}/E_{\mathrm{T}} \approx 1$. They also manually removed events were jets or limited detector coverage contributed to the missing tranverse momentum. This led 6 UA1 and 4 UA2 events. The UA1 collaboration considered three sources of background. The one produced due hadrons was eliminated by rejecting tracks with hadronic signature. The number of electron pair production and missing one was nearly zero. And the last was due to heavy flavour production that decay semi leptonic. The signature would just be the same if all other particles would have been missed, which is extremly unlikely. This led to the conclution that no background process could produce the 6 reminding events. In both cases the events were considered as the discovery of the w boson with a mass off

$$m_W = 81 \pm 5\,\mathrm{GeV} \ \ (\mathrm{UA1}) \qquad\qquad m_W = 80^{+10}_{-6}\,\mathrm{GeV} \ \ (\mathrm{UA1})$$

Both collaboration also fitted a theory prediction assuming a V-A coupling for the W boson to the tranverse W momentum (UA1) or $E_{\mathrm{T}}(\vartheta)$ (UA2) distribution which in both cases fitted the data.

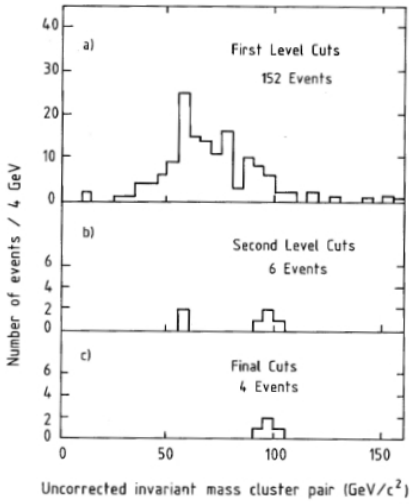

Figure 11: Invaraint mass distribution of the lepton pairs after subsequent cuts in the UA1 analysis.[11]

Again both collaborations searched for the same decay $Z^0 \rightarrow l^+l^-$. The search of the UA2 collaboration was detector specific and led to 4 consistent e^+e^- events. The UA1 experiment had a different analysis strategy. First they requiered two electromagnetic cluster, where each has 25 GeV or more. This led to 152 e^+e^- evnts. Requiering isolated tracks with a tranverse momentum of $p_{\mathrm{T}} > 7\,\mathrm{GeV}$ led just 6 remaining events. The third and last step was that less than 800 MeV show up in the hadronic calorimeter to suppress the hadronic background. In the end the UA1 collaboration found 4 e^+e^- events and 1 $\mu^+\mu^-$ event. These led to the discovery of the Z boson with an mass of

$$m_Z = 92.5 \pm 2.5(\mathrm{stat.}) \pm 3.0(\mathrm{syst.})\ \mathrm{GeV} \ \ (\mathrm{UA1})$$
$$m_Z = 91.9 \pm 1.3(\mathrm{stat.}) \pm 1.4(\mathrm{syst.})\ \mathrm{GeV} \ \ (\mathrm{UA2})$$

In 1984 C.Rubbia and S. van der Meer were awarded with the Nobel prize for their work leading to the discovery of the W and the Z boson. Shortly after this discovery CERN began to opperate the LEP collider. Since lepton colliders provide cleaner events with far less jets, it was possible to perform high precision measurements that were all consistent with the SM. The measurement of the W mass at the LHC is far more challening for example due to the large number of interaction per beam crossing. Never the less the uncertainties have been further reduced. The weak sector is still an interesting topic since e.g. FCNC are one of the few measurments that show tensions to the SM predictions.

10 The discovery of the top quark [12]

After the discovery of the b-quark at Fermilab in 1977, the search for the t quark started. It was the last missing particle to confirm the six-quark model, which is the foundation of the CKM matrix. Numerous experiments at e^+e^- collidern and the SppS were just able to set lower limits for the top quark mass. It was finally discovered at the Tevatron in 1995.

10.1 Theoretical predictions

The top quark is with a mass of $m_t = (173.0 \pm 0.4)$ GeV, the heaviest particle of the Standard Model. It has a charge of $\frac{2}{3}$e and a very short mean lifetime of $\tau = 0.5 \cdot 10^{-24}$ s. The lifetime is so short, that the t quark mainly decays into a W boson and a b quark ($V_{tb} = 1.019 \pm 0.025$), before hadronization can occur. This maximal transition probability is also the reason that single top quark production always occurs with a b quark or a W boson. The pair production of top quarks is always associated with gluons. Due to the short lifetime the information about the spin correlation of the $t\bar{t}$ pair remains and is preserved in the angular distribution of the decay products. In general the t quark can decay dileptonic, semi-leptonic or hadronically, whereby the dileptonic the cleanest event channel is. The high mass of the top quark is a result of the Yukawa coupling of $Y_t \approx 1$. For this reason the Higgs boson prefers to couple to the t quark. Under the assumption that BSM physics is above the SM energy scale, it couples highly to mass and therefore the top quark should be sensitive to it.
It was possible to predict lower limits for the top quark mass with lepton colliders, since top quark loops are corrections to the weak boson masses. The loop corrections depend on the mass of the circulating particle. Therefore it was possible to extract predictions for the t quark mass from electroweak precision measurements.

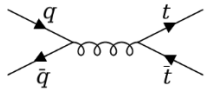

Figure 12: $t\bar{t}$ production via $q\bar{q}$ annihilation. [12]

For hadron collider the production process of top quarks highly depends on the center of mass energy. Parton distribution functions (PDF) $f_i(x_i, \mu_F^2)$ describe how large the probability is to observe a specific parton i with the momentum fraction x_i. μ_F^2 is the factorization scale and corresponds to the center of mass energy. PDFs are the results of measurements and cannot be calculate with pertubative quantumchromodynamik. With increasing energy a proton contains a continously growing amount of $q\bar{q}$ pairs, the sea quarks, due to quantum fluctuations and after a certain point is dominated by gluons. For the energies of the Tevatron are the quark distribution functions much larger than that of the gluon. This is the reason why 90 % of the events occur due to quark-antiquark annihilation. While for the LHC 90 % of the events occur due to gluon fusion.

Measurements

The Tevatron was part of Fermilab's accelarotor chain and was a hadron collider. The experiments CDF and DØwere placed at the two collision points. Besides the top quark, the bottom quark and the tau neutrino were discovered at the Tevatron. The Tevatran had a circumference of 6.3 km and accelaroted protons up to nearly 1 TeV. In 1995, the year of the top quark discovery it was operated with a center of mass energy of $\sqrt{s} = 1.8$ TeV.

10.2 The CDF Experiment

The CDF experiment contained a magnetic spectrometer surrounded by calorimeters and muon chambers. The Silicon vertex detector was used to reconstructed tracks of charged particles. The central outer tracker was a gas filled chamber to determine the particle momenta. Both parts were surrounded by a superconducting solenoid. Outside of the magnet were the electromagnetic calorimeter followed by the hadronic calorimeter and the most outer part was the muon detector. It was used to

measure the muon position and its time.
The discovery channel of the CDF experiment was $t\bar{t} \to WbW\bar{b}$, which then decays into two opposite charged leptons and to b jets or semiletonic in one lepton and at least four jets. Therefore they requiered an isolated lepton with $p_{\mathrm{t}} \geq 20\,\mathrm{GeV}$ and at least one b-tagged jet. They also removed dilepton events with a invariant mass between 75 and 105 GeV to exclude the pole of the Z boson. In 1995, they reached a luminosity of $\mathcal{L} = 67\,\mathrm{pb}^{-1}$, which allowed the discovery of the top quark.

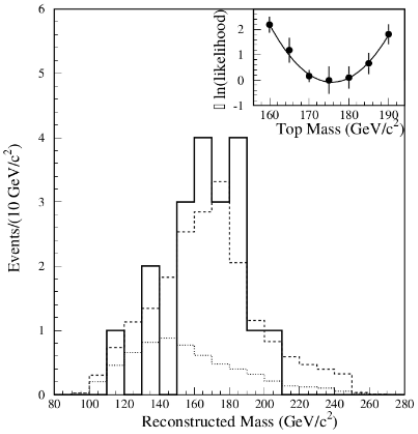

Figure 13: Invaraint mass distribution measured by the CDF to determine the top quark mass.[12]

The collaboration considered several backgrounds for example hadrons misidentified as leptons or the production of WW or $b\bar{b}$ events. They used to different taggers to reduce the background in the semileptonic decays. The secondary vertex algorithm tagged an event, if it finds a secondary vertex belonging to a b jet. The soft lepton tagger searched for additional leptons semileptonic decays of b jets. The tagging reduced the number of events per amount of jets much closer to the expected number of background tags.
Figure 13 shows the reconstructed mass dirstribution for b-tagged measurements with more than 4 jets and the performed likelihood fit to determine the top quark mass. The dotted line shows the background (BG) shape and the dashed line it the sum of $t\bar{t}$ + BG Monte Carlo events. The best fit mass, after studies of the systematic uncertainties is: $m_t = 176 \pm 18$ GeV.

10.3 The DØExperiment

At the DØ experiment reached a luminosity of $\mathcal{L}$ 44-56 pb^{-1}. For the analysis they defined the variable H_t as either the scalar sum of transverse energies E_T of jets for a single lepton and $\mu\mu$ + jets, or of leading eletron and jets for $e\mu$ + jets or ee + jets events. They considered different backgrounds for the dilepton channel: Z and Drell-Yan lepton pairs, the production if the vector boson pairs WW or WZ, or the heavy flavour production $b\bar{b}$ and $c\bar{c}$. The last considered background was due to jets misidentified as leptons. The variable H_t was used as a discriminator between background and signal. They also observed a statistically significant excess of events and reconstructed the top quark mass to be $m_t = 199 \pm 42$ GeV.

Outlook

In the past years the ATLAS and CMS collaboration have carried out high precision measurements of the top quark mass with significant reduced uncertainties. This is possible since the higher center of mass energy of the LHC allows to collect more data and therefore accesses higher statistics. The goal of high precision measurements is to reach a higher sensitivity for possible BSM physics. Other measurements that a carried out are for example the measurement of the spin correlation or the mass asymmetry of $t\bar{t}$ pairs. The latter enables the possibility to measure the CPT invariance.

11 The Discovery of the Higgs Boson [13]

The discovery of the Higgs boson was finally anounced on the 4th of July 2012. The ATLAS and CMS collaboration both confirmed the discovery of a Higgs like particle. The discovery of the Higgs boson closed some serious question of the Standard Model like the origin of mass.

11.1 Theoretical principle

The Standard Model describes the properties and interaction of elementary particles with gauge theories. It was experimemtally determined, that several particles carry a mass. The problem is that the electroweak symmetry requieres massless particles, since the explicit mass terms would break it. The solution was found in 1964 by proposing the Higgs mechanism. The Higgs field Φ is a isospin doublet of complex scalar fields:

$$\Phi = \begin{pmatrix} \Phi^+ \\ \Phi^0 \end{pmatrix} = \frac{1}{\sqrt{2}} \begin{pmatrix} \Phi_1 + i\Phi_2 \\ \Phi_3 + i\Phi_4 \end{pmatrix} \qquad < \Phi >= \frac{1}{\sqrt{2}} \begin{pmatrix} 0 \\ v \end{pmatrix} \text{ with } v = \sqrt{-\frac{\mu^2}{\lambda}}$$

The Higgs potential is a mexican hat potential and therefore the electroweak symmetry is spontanously broken. The initial Higgs field has four degrees of freedom, after the SSB three are observed by the weak gauge boson masses and the forth leads to the Higgs Boson. The development around the minimum leads to explicit mass terms for the gauge bosons $W^{\pm}$ and Z^0. In addition do the fermions get their masses by the Yukawa interaction and couple to the Higgs Boson.
The Higgs boson is a scalar with Spin 0. It couples to all particles proportional to their mass and due to the selfcoupling term gets a mass itself. Due to the high mass it has a short lifetime. The Higgs boson can be produced as fussion or radiation of massive particles since it couples to mass. The highest production of the Higgs boson is due gluon fusion, that couple couple to a quark loop or decay into a $q\bar{q}$ pair. But even under the LHC conditions the probability for Higgs production is extrem small. There is just one in 10^9 events. In principle the Higgs boson can decay in every massive particle, but the upper limit is $m_H \approx \frac{m^2_{decay}}{2}$. There are also decays into $Z\gamma$ or gg possible over loops. The problem was, that the branching fraction highly depends on the actually mass of the Higgs boson and many channels have a high background.

11.2 Statistics

The Higgs boson creates an signal excess at a specific invariant mass. Due to the high backgrounds that can also fluctuate, it is important to evaluate the significance of the signal. Different terms from the statistics are important to understand why the discovery of the Higgs boson was possible.
The signal strength μ is directly connected to the counting rate $n = \mu(\text{signal}) + \text{background}$ and defined by $\mu = \frac{\sigma(m_H)}{\sigma_{\text{SM}}(m_H)}$. A hypothesis gives the probability of a set of possible results. The *p-value* gives the proporbility for the excess to be generated by fluctuation with the hypothesis that there is no signal. The smaller the the p-value is the less likely it the hypothesis. The *level of significance* is a chosen level α to reject the hypothesis for $p < \alpha$. The *confidence interval* contains the true calues with a specific value. In particle physics the usually chosen *confidence level* (CL)is 95 % CL. This allows to set limits based on measured data with a specific CL. The Likelihood ratio $q_0 = -2\log\left(\frac{L(BG)}{L(\mu S+BG)}\right)$ can be used to reject a hypothesis if $q_0 > \alpha$, but it is not reliable for low sensitivity experiments since the distributions are too similar.
For the CL_s method are two pdfs of the test statistic Q created with a fixed mass hypothesis. One distribution is created with the background and one with the background with signal hypithesis. Afterwards the p value of both distributions is calculated respectivley to the observed $Q_{/textobs}$. The

signal confidence value is thus $CL_s = \frac{p(S+BG)}{1-p(BG)}$. The signal-background hypothesis is rejected at 95 % CL for $CL_s \leq 0.05$.

11.3 Previous results

The CDF and DØ collaborations at Tevatron set the Higgs mass limits to be either $m_H < 162\,\text{GeV}$ or $m_H > 166\,\text{GeV}$ at 95 % CL. The experiments at the LEP collider performed χ^2 tests to precision measurements of electroweak observables. This allows to extract mass limits for m_H, since the the Higgs boson contributes in loop corrections to the electroweak propagator. The best fit value was between 95 and 105 GeV, but this region was already excluded by direct searches. Together with other results from direct searches the limit was set to $m_H < 158\,\text{GeV}$.

11.4 The Discovery at the LHC

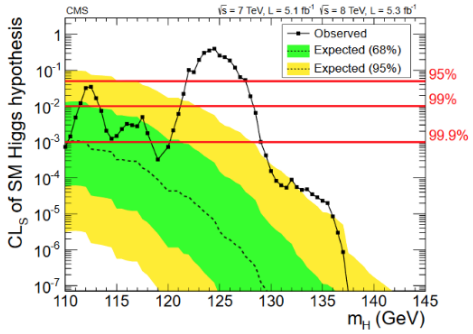

Figure 14: CL_s text for the Higgs boson mass hypthesis of $m_h \approx 125\,\text{GeV}$. [13]

The LHC is a 27 km hadron collider build to discover the Higgs boson. The LHC contains two general purpose detectors, ATLAS and CMS, with the main goal to find the Higgs boson. Their physics programme contains also the search for new physics i.e. SUSY particles. The idea was to build two experiments to independently valid the results and minimize systematic uncertainties with different detector designs. Both experiments conatin a tracking system, a solenoid, calorimeter and muon detectors. The main difference is that ATLAS placed the solenoid before the calorimeters, while CMS placed the solenoid behind them. ATLAS and CMS mainly concentrated on the two channels $H \to ZZ^* \to 4l$ and $H \to \gamma\gamma$ since they have the best properties. Other channel have a significant large background due to undetectable neutrinos or QCD processes that produce further jets.
Both collaborations could exclude masses above 129 GeV, but had no signifcant excess around 125 GeV with the data from the run 2011. The LHC increased the center of mass energy in 2012 from 7 TeV to 8 TeV. This led to a higher luminosity and increased the production cross section. Both collaborations beformed CL_s tests at a 95 % CL. ATLAS could not exclude $122 < m_H < 131\,\text{GeV}$ and CMS $122 < m_H < 131\,\text{GeV}$ at the 95 % CL. Together with the 2011 and 2012 data sets they finally reached significant excess and published the dicovery of a Higgs like particle with 5.9(ATLAS) and 5.0 (CMS) standard deviations in Juni 2012. The new scalar had a mass of

$$m_H = 126.0 \pm 0.4 \pm 0.4\ \text{GeV} \quad \text{(ATLAS)}$$
$$m_H = 125.3 \pm 0.4 \pm 0.5\ \text{GeV} \quad \text{(CMS)}$$

More measurements of different properties have been performed to confirm that the new found particle is indeed the Higgs boson. They proved the linear couling of the Higgs to massive elementary particles. By determining the new particle to be a spin 0 boson in 2013, they finally anounced that it was indeed the Higgs boson. The most precise measurement is $m_H = 125.10 \pm 0.14\,\text{GeV}$. In Oktober 2013 Higgs and Englert were awarded with the Nobel prize for providing the theory of the Higgs mechanism.

12 The Discovery of Three Types of Neutrinos [14]

The discovery of all three types of neutrinos took nearly 50 years. It was again a success of the Standard model, that for example predicted the ν_τ 25 years before it was finally discovered in 2000.

12.1 Fermi's Theory

In 1930 Pauli predicted the neutrino to explain the observed electron energy spectrum of the β decay. In 1934 Fermi developed his theory of the β decay based on Dirac's quantum field theory of electromagnetism. Since the weak force has a short range, he proposed a point like interaction to transfer the electric and weak charge between the two currents. These are build out of the two interacting particles of the initial and final state. The coupling strength G_F is valid for all processes of this form, since they are based on the same interaction. The crossing symmetry allows processes to be rearragend. The β decay of the neutron $n \to p + e^- + \bar{\nu}_e$ can therefore be transfromed to the inverse β decay $p + \bar{\nu}_e \to n + e^+$. This process was important for the detection of neutrinos.
Today we know that a $W^\pm$ boson is exchanged between the to currents in the β decay. The short range of the weak interaction is a result of massive gauge bosons. The third boson Z^0 of the weak interaction does not change the flavour of the current as the $W^\pm$ do. Fermi's theory did not predict the bosons and is therfore just valid on short distances. This manifests itself in the massdimension of the coupling strength G_F.

12.2 Discovery of the electron neutrino

The principle of spin conservation lead to the conclution that the neutrino is a fermion with spin $\frac{1}{2}$. It was already known from the discovery of the positron and the antiproton, that all fermions have corresponding antiparticles. Since there was no measurement of a mass or a magnetic moment, it remained unclear if the neutrino is a Dirac or Majorana particle. The latter is a particle that is its own antiparticle. The nature of the neutrino is under investigation by the search of neutrinoless double β decay. If the neutrino is a Majorana particle it would reabsorb itself and the neutrinos would vanish in the decay $^{150}Nd \to {}^{150}Sm + 2e^- + 2\bar{\nu}_e$.
The cross section of neutrinos could be calculated, because the β energy spectrum and G_F were known. The problem was that $\sigma_\nu \propto 10^{-44}$, this leads to an infinite matter penetrability for low energy neutrinos, where their energy is smaller as the reaction treshold. The penetrability is still large for MeV neutrinos. The first idea was to use the inverse β decay and detect the positrons and neutrons, that are produced. A large fussion reactor could provide a high rate of antineutrinos, but a reasonable signal to background rate is needed, to discover the neutrino.
The first attempt took place at the Hanford experiment with a plutonium-producing fission reactor in 1953. It contianed a 300-liter liquid scintillator to provide the protons. Since the mean free path of the neutron is longer as the positron ones, they measured the time delay between two signal. They estimated the delay to be approximate 9 µs to be an antineutrino signal. But they did not measured a significant signal to background rate, because they underestimated the influence of cosmic rays.
The Savannah River experiment finally lead to the discovery of the electron neutrino. It was placed deep underground and surrounded by a lead-paraffin shielding to minimize the influence of cosmis rays. It is made out of three tanks with a liquid scintillator inside and photomultipliers at the ends. Between these three scintillator tanks are two tanks placed, that contain a target solution out of water and cadmium chlorid. If a neutrino enters the tank and hits a proton the positron and neutron are produced. The positron annihilates nearly immediately with an electron under the emission of two 0.511 MeV photons. Due to longer free path the neutron remains longer till it is captured by the cadmium under the emission of a 9 MeV photon energy. The three detector tanks are connected to one input of a triple-beam oscilloscope. Two pulse heights with the correrponding energy of the

two processes and a time delay of 5.5 µs need to be measured to be counted as a signal. Due to the geometric of the experiment the signal also shows up in two read-out signals. This lead to a signal to background ratio of 3 to 1 and was awarded in 1995 with the Nobel prize as the discovery of the electron (anti-)neutrino.

12.3 Discovery of the Muon Neutrino

Under the assumption of two different kind of neutrinos, they only produce the corresponding lepton e.g. $\nu_e/\bar{\nu}_e \to e^-/e^+$. In this case the charged pion decays into lepton and the corresponding neutrino. Since the electron mass is much smaller as the muon mass, the decay into an electron and the ν_e is helicity supressed. Pontecorvo and Schwartz proposed independently to use particle accelerators to search for the muon neutrino. The Brookhaven Alternating Gradient Synchrotron (AGS) had an alternating magnetic field to focus the proton beam even at high energies. The resulting 15 GeV beam was collided with a beryllium target on a straight section. This produced pions with a small angle respectively to the synchroton ring, that afterwards mainly decayed into muons and neutrinos. The spark chamber detector was shield with steel from the main background, strongly interacting particles and muons. The detector consists of 10 one-ton modules, that are build out of 9 aluminium plates seperated by lucite spacers. The shielding made it impossible to produce neutron events. The collaboration observed 24 single muon events, where 5 got exclude, because they did not origin from the AGS. They could have been cosmic rays. If only one type of neutrino exists the collaboration also need to detect 29 electron showers. Instead they just observed 6 possible electron showers. This lead to the discovery of the muon neutrino in 1962.

12.4 Discovery of the Tau Neutrino

After the discovery of the τ and ν_μ, the τ neutrino was predicted as a third neutrino generation. The τ neutrino was discovered by the DONUT collaboration in 2000. They used the collision of a 800 GeV proton beam with a target to produce D_s mesons, that are heavy enough to decay into τ leptons and ν_τ neutrinos. The decay into the ν_τ is helicity supressed compared to the τ. Between the target and the detector is a shielding in order to ensure just neutrinos pass trough. The detector is composed out of three iron blocks which are seperated with a plastic layer between two emulsion layers. The principle that lead to the discovery of the τ neutrino was, if a ν_τ collides with a iron nucleus, it produces a τ lepton which decays afterwards. By detecting the τ lepton with the emulsion layers, the collaboration indirectly proved the existence of the τ neutrino.

12.5 Number of light neutrinos

The Z production at e^+e^- collidern allows to precisely measure the number of light neutrinos. By subtracting the visible partial decay width Γ_{vis} of the Z boson into charged quarks and leptons from the total Z decay width the partial decay with Γ_{inv} into neutrinos reminds. This can be used to calculate the number of neutrinos N_ν as following:

$$N_\nu = \frac{\Gamma_{\text{inv}}}{\Gamma_l}\left(\frac{\Gamma_l}{\Gamma_\nu}\right)_{\text{SM}} \qquad \left(\frac{\Gamma_l}{\Gamma_\nu}\right)_{\text{SM}} = 1.991 \pm 0.001 \; .$$

The results of all four LEP experiment lead to $N_\nu = 2.984 \pm 0.008$. Therefore the ν_e, ν_μ and ν_τ are all light neutrino generations predicted by the Z decay width.

13 Neutrino Oscillation [15]

Neutrino oscillation are a direct consequense of the fact that neutrinos have masses. Several experiments had observed neutrino deficits for the solar and atmospheric neutrinos. The Super-Kamiokande and the Sudbury-Neutrino-Observatory made it possible to prove that these are caused by neutrino oscillations.

13.1 Historical Context

In 1957 Pontecorvo proposed neutrino oscillations for the first time. In 1962, the same year as the muon neutrino discovery, the PMNS matrix was introduced. It provided a framework to explain possible neutrino oscillations.
Since the neutrino cross section is $\sigma_\nu \sim 10^{-14}\mathrm{b/GeV}$ alarge and predictable flux of neutrinos is needed for experiments with neutrinos. The most suitable ones are solar and atmospheric neutrinos. The solar neutrinos are only electron neutrinos that are produced by nuclear fusion in the pp chain reaction. The Standard Solar Model (SSM) by Bahcall made it possible to predict the steady flux. The β^+ decay of the ^8B provides neutrinos with the highest energy of up to 18.8 MeV, but the flux is also the lowest. The first experiment investigating the solar neutrino flux was the Homestake experiment. It was developed in the 1960s by R.Davis and placed in the Homestake mine 1478 m underground. The detector was a tank of perchloroethylene, that is able to detect neutrinos with an energy above 0.814 MeV. The by the reaction $\nu_e + ^{37}C \rightarrow e^- + ^{37}Ar$ produced Argon was extracted and its decays counted. This lead to the discovry that only about one-third of the preticted SSM neutrinos reach the earth. When a cosmic ray hits the atmosphere it creates a shower that contains pions. The pions decay into muons which in turn decay into electrons. The expected ratio of the atmospheric neutrinos is $\frac{\nu_\mu}{\nu_e} \approx 2$. The Kamiokande experiment was build to search for the proton decay. Muon neutrinos are the main background. In 1988 the Super-Kamiokande experiment published their result of the ratio $\frac{(\nu_\mu/\nu_e)_{\mathrm{exp}}}{(\nu_\mu/\nu_e)_{\mathrm{theo}}} = 0.60 \pm 0.05$, which indicates a atmospheric neutrino deficit. This result was later confirmed by the IMB experiment.

13.2 Theoretical principles

Assuming that neutrinos carry a mass, their flavour eigenstates (ν_i with $i = e.\mu, \tau$) are different from the mass eigenstates (ν_j with $j = 1, 2, 3$). The PMNS (Pontecrovo-Maki-Nakagawa-Sakata) matrix U describes the mixing of the mass eigenstates into the flavour eigenstates. U is a 3 mixing matrix containing three real mixing angles and one complex phase factor.
The propagation of a mass eigenstate can be described by $|\nu_j(t)\rangle = e^{-iHt}\,|\nu_j(0)\rangle = e^{-iEt}\,|\nu_j(0)\rangle$, where the Hamiltonian operator is equivalent to the initial energy carried by the neutrino. It is the solution of the time-dependent Schrödinger equation described by the Hamiltonian operator in vacuum. The flavour eigenstate is then given by $|\nu_i(t)\rangle = \sum_i U^*_{ij} e^{-iH_i t}\,|\nu_j(0)\rangle$.
In the simplified scenario of two neutrino times, the oscillation probabilty between tweo flavour eigentstates is given by:

$$P(\nu_{F1} \rightarrow \nu_{F2}) = |\langle \nu_{F2} | \nu_{F1} \rangle|^2 = \sin^2 2\vartheta \sin^2 \frac{\Delta m^2 L}{4E}\ .$$

Here is ϑ the mixing angle that affects the amplitude and $\Delta m^2 = m_2^2 - m_1^2$, which effects the frequency. Current measurments discovered thatthe mic´xing in the PMNS matrix is nearly maximal. Moreover, only the mass differences, but not the masses themselves, could be determined so far. They are $|\Delta m^2_{21}| = 7.55^{+0.20}_{-0.16} 10^{-5}\mathrm{eV}^2$ and $|\Delta m^2_{31}| = 2.50^{+0.03}_{-0.03} 10^{-3}\mathrm{eV}^2$.

13.3 Super-Kamiokande

The motivation for the neutrino flux measurement of Super-Kamiokande was the fact that neutrinos can easily traverse the earth due to their small cross section. As shown before, depends the oscillation probability on the distance the neutrinos travel. The upward and downward going neurtinos cover significant different distances. So if the observed anomaly is due to oscillation, the flavour composition of the neutrino flux should depend on the angle.
Super-Kamiokande is a cylindrical Cherenkov Detector that contains 22 500 t of ultra pure warer and 11 146 Photomultipliers. The neutrinos interact weakly with a nucleus and produce a charged lepton. Electron events are smeared out compared to the muon events due bremsstahlung effects. In 1998 the collaboration published the first significant evidence for atmospheric neutrino oscillation. They reported a significant zenith dependent deficit of the μ-like events compared to the probability of no oscillaitons. The channels of the ν_e and the downward going ν_μ events were in agreement with the expactation of no oscillation. This behavior has been seen in the sub-GeV and multi-GeV sector. The ratio $R = \frac{(\mu/e)_{\text{Data}}}{(\mu/e)_{\text{MC}}}$ was $R = 0.63 \pm 0.05$ (sub-GeV) 0.65 ± 0.08 (multi-GeV). The data have been consistent with the two flavour ν_μ, ν_τ oscillation.

13.4 The Sudbury Neutrino Observatory

The Sudbury Neutrino Observatory (SNO) was build to investigate the nature of the solar neutrino deficit. Possible sources could be neutrino oscillation, a neutrino decay or that the SSM is incorrect. In contrast to previous experiments the SNO was not only sensitiv to ν_e, but also the sum of all neutrino types. This is due to the use of Deuterium as detector material. The SNO was Cherenkov detector, that was placed 2 km underground and contained over 9000 photomultipliers.
The neutrinos interact in three different ways:

- charged current (CC) interaction: $d + \nu_e \rightarrow \ p + p + e^-$ The neutrino energies reach up to 15 MeV, but the mass of the muon is much greater. This is the reason why the charged current reactions are just for electron neutrinos possible. ($\Phi_{\text{CC}} = \Phi(\nu_e)$) detektierbar.
- neutral current (NC) interaction: $d + \nu_x \rightarrow \ \nu_x + n + p$ This process is sensitive to all types of neutrinos. The neutron capture leads to a photon cascade, which can interact via compton or photo effect and produce high-energetic electrons. These produce Cherenkov light with an isotropic distribution. Hence it is possible to seperate NC and CC events. ($\Phi_{\text{NC}} = \Phi(\nu_e) + \Phi(\nu_{\mu/\tau})$)
- electron elastic scattering (ES): $\nu_x + e^- \rightarrow \ \nu_x + e^-$ The elastic scattering with a valence electron is far more senstitive to electron neutrino than to other types. It is strongly correlated to the neutrino direction. ($\Phi_{\text{ES}} = \Phi(\nu_e) + 0.1559\Phi(\nu_{\mu/\tau})$)

The angular distribution showed a slightly anticorrelation for the CC, a strong correlation for the ES and no correlation at all for the NC to the angle of the neutrinos. The measured fluxes are

$$\Phi_{\text{CC}} = 1.76^{+0.06}_{-0.05}(\text{stat.})^{+0.09}_{-0.09}(\text{syst.})\Phi_{\text{NC}} \quad = 2.39^{+0.24}_{-0.23}(\text{stat.})^{+0.12}_{-0.12}(\text{syst.})\Phi_{\text{ES}} = 5.09^{+0.44}_{-0.43}(\text{stat.})^{+0.46}_{-0.43}(\text{syst.})$$

All fluxes counted together fit the predicted flux of the SSM. Together with the measurment of a significant flux of $\nu_{\mu/\tau}$, this was the confirmation the the solar neutrino deficit is due to neutrino oscilations.
The discovery of neutrino oscillation was an important step in neutrino physsics. It proved that neutrinos have a mass and opened the question of the mass hierachy and the absolute masses of the neutrinos. Other unsolved problems are the nature of the neutrino masses, the CP violation in the leptonic sector or the search for sterile right-handed neutrinos. This problems will be investigated with future experiments like KATRIN (masses), Hyper-Kamiokande (CP violation) and SNO+ (mass nature).

References

[1] Christopher Krause. *Cherenkov Detectors*. 22.11.19.

[2] Serena Di Pede. *Semiconductor Detectors*. 31.01.20.

[3] Edifici Eureka. Campus UAB. *Alibava Systems Activity Book For Students - First editon*. URL: `https://www.alibavasystems.com/images/EASy-exercises/EASY-Exercise-Book.pdf` (visited on 02/15/2020).

[4] Janina Nicolini. *The Wu Experiment*. 25.10.19.

[5] Lars Röhrig. *The Goldhaber Experiment*. 06.12.19.

[6] Janis Sowa. *Discovery of Neutral Current*. 24.01.20.

[7] Janina Nicolini. *Seminar Falsche Entdeckungen: Die Entdeckung der Neutralen Ströme*. 27.06.19.

[8] Jonah Blank. *The Discovery of CP Violation*. 17.01.20.

[9] David Rolf. *$B\bar{B}$ Oszillation*. 20.12.19.

[10] Michael Windau. *The Discovery of the Gluon*. 08.11.19.

[11] Jan Lukas Späh. *The Discovery of W and Z Boson*. 10.01.20.

[12] Nicole Schulte. *Discovery of the Top Quark*. 29.11.19.

[13] Miriam Schwarze. *The Discovery of the Higgs Boson*. 06.12.19.

[14] Jan Ellbracht. *The Discovery of Three Types of Neutrinos*. 22.11.19.

[15] Lara Nollen. *Neutrino Oszillation*. 13.12.19.